We are grateful to the editor and reviewers for the time they devoted to reviewing this manuscript and for the constructive comments, all of which were taken into account in the revised manuscript. Below, we address all comments point by point. The comments are reproduced in blue, and the authors' responses are provided in black. The underlined text indicates our corresponding changes in the revised manuscript and in the updated supporting information, both of which are provided with tracked changes. The locations of the underlined text are highlighted in **bold black text**.

Key revisions to the manuscript include:

- The manuscript title was revised to explicitly indicate the 23-year study period and clarify the temporal resolution (8 days) of the dataset.
- The Introduction was substantially updated with Antarctic-specific studies on supraglacial lake monitoring, meltwater impacts on ice dynamics and ice-shelf stability, and melt–albedo feedback. c
- The Methods section was substantially reorganized into seven subsections corresponding to the processing stages in Fig. 2.
- The Sentinel-2 reference data extraction procedure was described in greater detail in Sect. 3.1, including manual sample labeling, three-class Random Forest (RF) classification, training and validation sample selection, and class-specific accuracy assessment.
- More details were added to the model development, optimization, and postprocessing procedures (Sects. 3.4 and 3.7), including hyperparameter grid search, five-fold cross-validation, independent testing, and the application of surface melt and historical lake extent constraints with spatial and temporal consistency criteria.
- The accuracy assessment in the Results and Discussion section was expanded to focus more explicitly on SGL fraction retrieval. Additional metrics, including bias and mean absolute error (MAE), were incorporated for a more comprehensive evaluation of retrieval accuracy.
- The Results and Discussion section was expanded to better connect the dataset findings with previous glaciological studies. Additional discussion was provided on SGL persistence, spatial distribution, seasonal evolution, and interannual variability. The potential influence of cloud contamination on long-term estimates was also discussed, and corresponding cloud masks were made available as auxiliary data.
- Figures 1–8 were redrawn, and Table 2 was revised.
- New figures and tables were added to the Supporting Information.

Author Response to Reviewer #2

Review

This is a novel paper which directly addresses the classic "mixed-pixel" dilemma of tracking small, highly dynamic features (supraglacial lakes, SGLs) using moderate-resolution satellite sensors. The workflow shown in Fig. 2 and described in Section 3 seems sensible and robust. I liked the two-stage hierarchical modelling (RFC + RFR) where, instead of forcing a single regression model to calculate fractions across the entire continent blindly, the authors first use a Random Forest Classifier (RFC) to binarize whether a pixel contains water and then pass it to a Random Forest Regressor (RFR) to compute sub-pixel fractions. This two-stage constraint should reduce false-positive noise in dry snow zones.

A vulnerability in many random forest papers is spatial autocorrelation (evaluating a model on pixels directly adjacent to the training pixels). The authors avoided this trap by reserving 7 completely independent geographic regions spanning multiple melt seasons exclusively for validation. Achieving an Overall Accuracy (OA) > 0.82 and an r > 0.73 on these unseen areas proves the model generalizes well.

Training the models using the high-temporal-resolution daily product (MOD09GA) matched to exact high-spatial-resolution Sentinel-2 passes, but deploying the final operational dataset on the 8-day composite (MOD09A1), is sound, logical and enables the production of pan-Antarctic maps of SGL area, persistence and fraction at 1 km resolution (Figs. 6–9), as well as time series averaged across regions of seasonal changes in SGL area showing how these vary over the 23-year record (Fig. 9).

The creation of a "Level 1" product that applies an active melt flux constraint (Zheng et al., 2025) and a historical spatial mask (Tuckett et al., 2025) also increases the robustness of the final datasets as it presumably goes some way to cleaning out false positives, for example due to cloud shadows that often slip past standard optical masks.

I have a few main points and lots of small, suggested edits/comments that I'd encourage the authors to consider.

AR1: We sincerely thank the reviewer for the positive and detailed assessment of our work. We appreciate the recognition of our two-stage RFC–RFR framework, the spatially independent validation strategy, and the integration of daily and 8-day MODIS observations. We are also grateful for the acknowledgment of the additional physical and spatial constraints used to improve the reliability of the dataset.

The reviewer's constructive comments and suggestions have helped us improve the methodological clarity, reproducibility, and presentation of the manuscript. We have

carefully considered each comment and revised the manuscript accordingly. Our detailed responses are provided below.

General comments

1.The current title is ambiguous and implies the dataset could be only 8 days long! If the authors want more people to read the paper, they should improve the title to convey that 8 day refers to temporal frequency, not the total duration of the dataset, e.g. "A 23-Year, 8-Day Temporal Resolution Antarctic Supraglacial Lake Dataset from MODIS."

AR2: We are grateful for your constructive recommendation. We agree that the original title could be misinterpreted as referring to a dataset covering only eight days. We have revised the title to explicitly indicate the 23-year study period and clarify that the 8-day interval refers to the temporal resolution of the dataset.

The revised title is as follows:

A 23-year, 8-day temporal resolution Antarctic supraglacial lake dataset from MODIS **(L1–2)**

2.I think the Methods section (Section 3) could be much improved. I'm not convinced someone could replicate the work from some of the descriptions given at present. I find it hard at times to reconcile what is written with the processing steps summarized in Fig. 2. I think the authors need to first outline the overarching methodology and refer broadly to the boxes and arrows of Fig. 2, for example clarifying that the RFC and RFR models are developed using the daily MODIS data, but that the final model works with the 8-day MODIS products. Then the authors need to go into more detail about each of the steps. It would be very helpful if seven subsections of Section 3 could map onto the seven stages of the workflow outlined in the seven boxes of Fig. 2 using the same names.

AR3: Thank you for this constructive comment. We agree that the original Methods section did not provide sufficient detail to fully explain the processing workflow and ensure reproducibility. We have therefore substantially revised and reorganized Sect. 3 to improve its clarity, completeness, and consistency with Fig. 2.

First, we have added an overview of the methodology to explain the overall workflow and its main processing stages. Second, we have reorganized Sect. 3 into seven subsections that correspond to the seven processing stages illustrated in Fig. 2, using consistent terminology and following the same sequence. We have also expanded the descriptions of the individual steps, including reference data preparation to make the

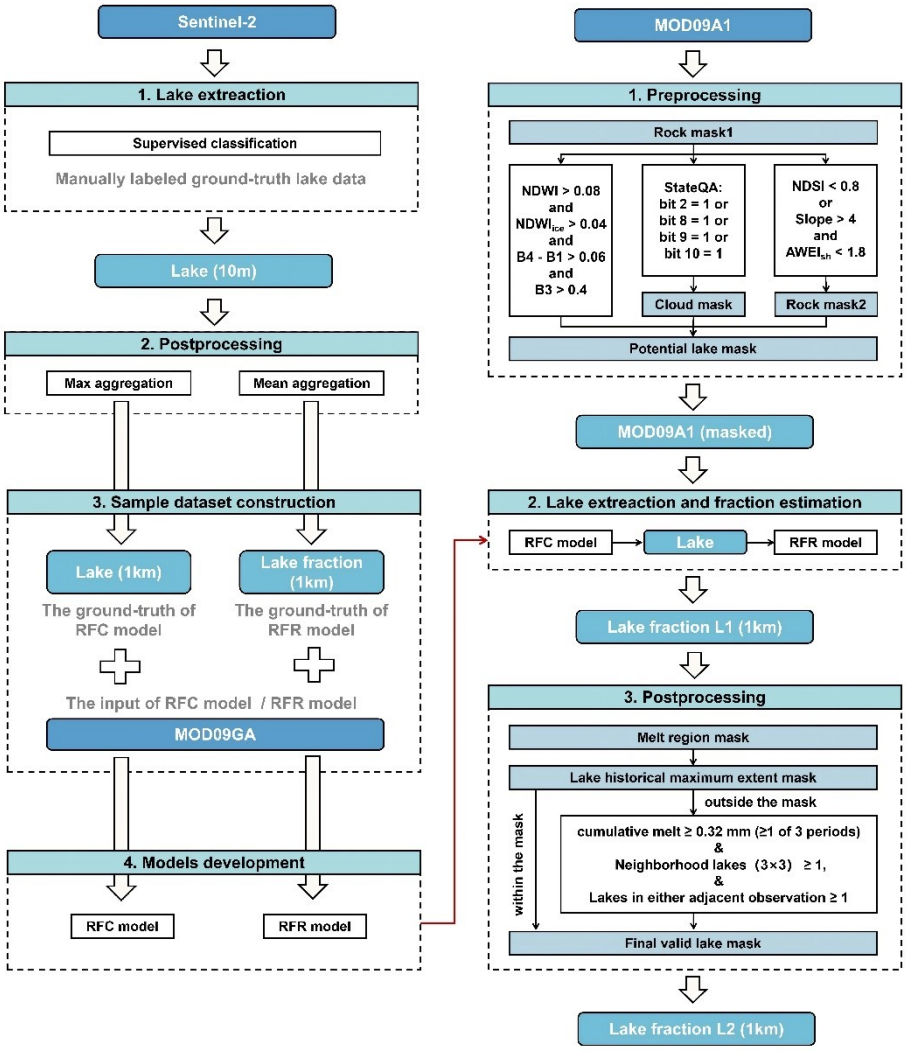
methodology easier to understand and reproduce.

The corresponding descriptions have been revised throughout Sect. 3, Methods.

3 Methods

Due to the relatively coarse spatial resolution of MODIS imagery, individual pixels often contain mixtures of lake and surrounding snow or ice, making it necessary to estimate the SGL fraction within each 1 km MODIS grid cell to accurately characterize SGL coverage across Antarctica. To address this issue, we incorporate high-spatial-resolution information from Sentinel-2 imagery into a two-stage machine-learning framework for dataset generation, in which a Random Forest classification (RFC) model is first used to identify SGL-containing pixels, and a Random Forest regression (RFR) model is then used to estimate the SGL fraction within each pixel. The Random Forest (RF) algorithm is an ensemble learning approach that builds on multiple decision trees and is known for its strong generalization capability (Breiman, 2001).

The overall workflow consists of seven stages organized into two interconnected components (Fig. 2). The first component comprises four stages for constructing "ground-truth" datasets from Sentinel-2 imagery and developing the RFC and RFR models using daily MOD09GA surface reflectance data. The second component comprises three stages in which the trained models are applied to 8-day MOD09A1 composite imagery to generate Antarctic-wide SGL fraction maps. The following subsections describe these seven stages in the order shown in Fig. 2.



130 Figure 2: Workflow of the Antarctic SGL fraction dataset generation from Sentinel-2 and MODIS imagery.

3.1 Lake extraction from Sentinel-2 imagery

High-resolution Sentinel-2 imagery is used to derive reference SGL data, corresponding to Step 1 ("Lake extraction") in Fig. 2. Sentinel-2 image selection is guided by previously reported SGL distributions (Corr et al., 2022; Kingslake et al., 2017; Stokes et al., 2019; Tuckett et al., 2025) and supplemented by manual visual interpretation. Images from multiple regions and melt seasons are selected to capture diverse SGL morphologies and surface conditions (Fig. 1 and Table S1).

140 For each selected Sentinel-2 image, an independent RF classifier is developed in GEE using nine spectral bands (B2–B8, B11, and B12) as input features (Breiman, 2001). Reference samples representing three surface features (lake,

slush, and ice) are manually labeled through visual interpretation of the imagery. These samples are randomly divided into training (70%) and validation (30%) subsets. Each RF classifier is trained on the training subset, while the validation subset is used to assess classification performance based on overall accuracy (OA), precision, recall, and F1-score (F1), with particular emphasis on the lake class. Only classification results meeting the predefined precision criterion (lake-class precision $\geqslant$ 95%) are retained. The classification performance metrics for individual Sentinel-2 images are summarized in Table S2.

The resulting three-class maps are converted into binary SGL maps, in which lake is labeled as 1 and slush and ice are labeled as 0. Separately classifying slush and lake helps reduce the misclassification of slush as lake. Sentinel-2 classification results are presented in Fig. S1.

3.2 Spatial aggregation of Sentinel-2 SGL maps

The extracted 10 m Sentinel-2 SGL maps are postprocessed to generate reference data at 1 km resolution, corresponding to Step 2 ("Postprocessing") in Fig. 2. To match the 1 km spatial resolution of MODIS imagery used in the machine-learning models, two aggregation strategies are applied. First, max aggregation is used to generate binary SGL labels at 1 km resolution. Under this strategy, a 1 km grid cell is labeled as an SGL pixel if at least one of its constituent 10 m pixels is classified as water. Second, mean aggregation is used to derive SGL fraction values at the same spatial resolution (Liang and Liu, 2021; McKenna et al., 2025). These values range from 0 to 1 and represent the proportion of each 1 km grid cell covered by SGLs. The resulting binary SGL labels and continuous SGL fraction values are subsequently used as reference data for the MODIS-based RFC and RFR models, respectively.

3.3 Construction of the MODIS–Sentinel-2 sample dataset

The SGL reference data derived from Sentinel-2 imagery are combined with MODIS surface reflectance data to construct a sample dataset for the two-stage machine-learning framework, corresponding to Step 3 ("Sample construction") in Fig. 2. Daily MOD09GA surface reflectance data, aggregated to a spatial resolution of 1 km, are used as model inputs, with seven spectral bands (B1–B7) serving as predictor variables. The corresponding binary SGL labels and SGL fraction values derived from Sentinel-2 imagery serve as reference outputs for the

RFC and RFR models, respectively. MODIS and Sentinel-2 observations acquired on the same day and covering the same regions are spatially matched to construct paired input and reference data at 1 km resolution.

Following quality assessment, a total of 26 sample regions are retained, from which approximately 5,000 lake samples and 10,000 non-lake samples are obtained. Of these, 19 regions are used for model training and validation, whereas the remaining seven regions are reserved for independent testing. These samples cover multiple Antarctic regions and melt seasons, allowing model performance to be assessed under different surface and environmental conditions (Fig. 1 and Table S1).

3.4 Random forest model development and optimization

The RFC and RFR models are developed in Step 4 ("Modelsc development") of Fig. 2, using the training samples described in Section 3.3. The RFC model combines multiple classification trees through majority voting to identify SGL pixels, whereas the RFR model averages predictions from regression trees to estimate continuous SGL fractions (Fig. 3). For both models, two key hyperparameters, the number of trees and the maximum number of leaf nodes per tree, are optimized using a grid search strategy (Bischl et al., 2023; Probst et al., 2019). The number of trees ranges from 5 to 200, while the maximum number of leaf nodes ranges from 5 to 100, both in increments of 5. Model performance is evaluated using five-fold cross-validation (Arlot and Celisse, 2010) on samples from 19 regions, while samples from the remaining seven regions are reserved for independent testing. The trained models can be applied to 8-day MOD09A1 composite imagery to map SGLs across Antarctica.

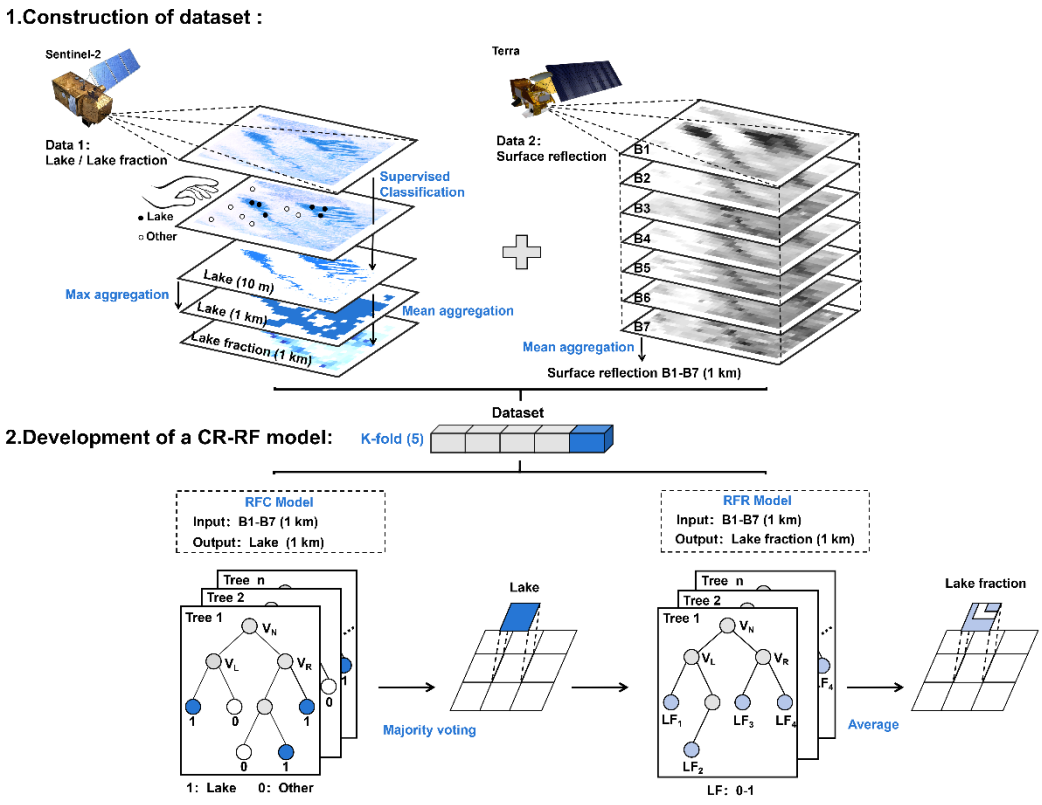


Figure 3: Architecture of the two-stage (RFC and RFR) model for SGL fraction estimation.

3.5 Preliminary screening of potential SGL pixels in MODIS imagery

The 8-day MOD09A1 imagery is preliminarily screened using spectral thresholds and auxiliary masks to identify potential SGL pixels for subsequent RFC-based classification, corresponding to Step 1 ("Preprocessing") in Fig. 2. The 8-day MOD09A1 composite product is used at this stage because it reduces cloud contamination and improves the stability of SGL retrieval compared with individual daily observations.

First, spatial masks are applied to exclude exposed bedrock areas. Potential lake pixels are then identified using a multi-threshold approach that exploits spectral contrasts between water, snow, and ice. Following Corr et al. (2022), two normalized difference water indices (NDWI and $NDWI_{ice}$) are used to identify candidate SGL pixels in MODIS imagery. NDWI uses the green and near-infrared bands to enhance open-water signals (McFeeters, 1996), whereas $NDWI_{ice}$ replaces green and near-infrared with blue and red, respectively, to better distinguish open water from surrounding snow, ice, and low-albedo slush (Yang and Smith, 2013). Combining these two indices improves the identification

of potential lake pixels, as their complementary spectral sensitivities help reduce ambiguity and misclassification under varying surface conditions. The two indices are calculated as follows:

$$NDWI = \frac{B4 - B2}{B4 + B2} \quad (1)$$

$$NDWI_{ice} = \frac{B3 - B1}{B3 + B1} \quad (2)$$

Due to the coarse spatial resolution of MODIS, SGLs may occupy only a small fraction of individual pixels, with surrounding snow and ice weakening the water-related spectral signals. To minimize missed detections of potential SGL pixels with low lake fractions, the NDWI and $NDWI_{ice}$ thresholds are empirically calibrated using reference lake samples derived from high-resolution Sentinel-2 imagery instead of directly adopting thresholds from previous studies (Text S1). The resulting thresholds are 0.08 for NDWI and 0.04 for $NDWI_{ice}$ (Fig. S2). Additional thresholds based on visible bands ($B4 - B1 > 0.06$ and $B3 > 0.4$) are applied to further refine the selection of candidate pixels (Moussavi et al., 2020). These thresholds help distinguish water from surrounding ice and snow surfaces, thereby improving SGL pixel identification.

However, NDWI-based classification may still lead to the misclassification of rock shadows and cloud-contaminated pixels as water. To reduce the misclassification of shadowed surfaces as SGLs, the Automated Water Extraction Index for shadow areas ($AWEI_{sh}$; Eq. (3)) and surface slope are used to exclude pixels with $AWEI_{sh}$ values below 1.8 and slopes greater than 4° (Feyisa et al., 2014).

$$AWEI_{sh} = B3 + 2.5 \times B4 - 1.5 \times (B2 + B6) - 0.25 \times B7 \quad (3)$$

In addition, cloud-contaminated and cloud-shadow-contaminated pixels are masked using the quality assurance bands provided with MODIS surface reflectance products (Ackerman et al., 1998, 2008). These preprocessing procedures are used to generate a potential lake mask that restricts the MOD09A1 pixels processed by the subsequent machine-learning models.

3.6 SGL extraction and fraction estimation using MOD09A1 imagery

The identification of SGL pixels and estimation of their lake fractions correspond to Step 2 (“Lake extraction and fraction estimation”) in Fig. 2. For the Antarctic

melt seasons from 2000 to 2023, each extending from early November to early April of the following year, the preliminarily screened MOD09A1 imagery is used as input to the trained RFC model to identify pixels containing SGLs. The model produces binary classification results (0 or 1), indicating the absence or presence of SGLs in each pixel. These classification results are then used as a mask to retain SGL-containing pixels, to which the trained RFR model is applied to estimate the SGL fraction within each pixel. The RFR model produces continuous SGL fraction estimates ranging from 0 to 1. The sequential outputs of the RFC and RFR models are illustrated in Fig. 3. The resulting SGL fraction maps form the initial Antarctic SGL fraction dataset.

3.7 Postprocessing of SGL fraction maps

The initial SGL fraction maps are further refined using constraints based on surface melt conditions and historical SGL distributions to improve their physical and spatial consistency, corresponding to Step 3 ("Postprocessing") in Fig. 2.

First, surface melt conditions are used as a physical constraint. Surface melt is widely recognized as a prerequisite for supraglacial lake formation (Leeson et al., 2012; Stokes et al., 2019). An independent Antarctic melt-flux dataset derived from Special Sensor Microwave/Imager (SSM/I) observations is used to constrain the retrieved SGL distributions (Zheng et al., 2025). For each 8-day SGL fraction image, daily melt flux is accumulated separately over three consecutive 8-day periods: the preceding, corresponding, and following periods. A melt mask is generated using a threshold of 0.32 mm, with pixels retained if the cumulative melt exceeds this threshold in any one of the three periods (Mätzler, 1996; Ulaby et al., 1981; Fig. 2). This temporal window accounts for potential differences between the timing of surface melting and SGL observations, reducing the omission of lakes that persist after active melting has ceased.

Second, a historical spatial constraint is applied to reduce misclassification caused by noise in MOD09A1 observations. A historical SGL distribution dataset derived from Landsat imagery for 2006–2021 (Tuckett et al., 2025) is used to generate a historical maximum SGL extent mask. Given the high temporal sampling frequency of MODIS observations, candidate lake pixels outside the historical maximum extent are not automatically removed. Instead, they are retained only when the spatial consistency criterion, temporal consistency criterion, and surface melt condition are all satisfied (Fig. 2). Specifically, the

spatial criterion requires at least one of the eight neighboring pixels within a 3 × 3 window to be classified as a lake pixel, while the temporal criterion requires the target pixel to be classified as a lake pixel in either the preceding or following 8-day observation. The resulting masks are applied to the retrieved SGL fraction maps to generate the final Antarctic SGL fraction product. **(L113–234)**

3.Building on Point 2, an example of where more detail is needed is the description of how the Sentinel-2 lakes were detected, which is currently exceedingly brief (L124–127). Reference is made to Niu et al. (2023) with no further detail. This is particularly concerning because the Sentinel-2 dataset is regarded as "ground truth" and so is the absolute anchor of the model developed in this study. If the training labels are flawed, the entire 23-year MODIS output inherits those flaws.

Furthermore, the text says the authors used "a supervised classification algorithm… (Niu et al., 2023)." Looking at the references, Niu et al. (2023) specifically developed a highly complex deep learning network (a U-Net with Attention Blocks). The authors should explicitly name the type of classifier (e.g., "an attention-based U-Net convolutional neural network") instead of using the generic umbrella term "supervised classification algorithm" and tell us more about it and how it was used in their study.

The authors state that "only images meeting the classification accuracy threshold (>95%) are selected." But unless I missed it, they do not explain how this 95% accuracy was calculated. Did they manually digitize independent validation polygons for every single one of the 26 Sentinel-2 scenes to run a confusion matrix? Who verified it?

The authors do not explain how the Sentinel-2 binary 1/0 map accounts for the real-world gradients of shallow water, deep water, and wet slush before it was averaged up to the 1 km scale. If the Sentinel-2 model mistook wet slush for open water (a classic problem), the MODIS regression model will consistently overestimate actual liquid lake volumes.

AR4: We appreciate your detailed and important comment. We agree that the reliability of the Sentinel-2 reference data is essential to the accuracy of the MODIS-based SGL fraction dataset. We also acknowledge that the original manuscript did not adequately describe the classification method, reference sample preparation, or accuracy assessment procedure.

In response, we have substantially revised Sect. 3.1. First, we clarify that our study uses a Random Forest (RF) classifier rather than the deep learning method proposed by Niu et al. (2023). We have removed the potentially misleading citation to Niu et al.

320 (2023) and added a detailed description of the Sentinel-2 image classification procedure. Second, we have clarified the preparation of reference samples and the accuracy assessment procedure, with particular emphasis on the lake-water class. Only classification results meeting the predefined precision criterion are retained. The classification metrics for individual Sentinel-2 images are now provided in Table S2. We further clarify that lake water, slush, and ice are classified separately before generating binary SGL maps. Subsequently, pixels classified as lake water are assigned a value of 1, whereas those classified as slush and ice are assigned a value of 0. Representative Sentinel-2 SGL classification maps have also been provided in Fig. S1. The corresponding revisions to Sect. 3.1 are detailed in **AR3.**

330 The classification accuracy metrics for individual Sentinel-2 images are presented in Table S2 of the Supplementary Information.

Table S2. Lake classification accuracy for 19 Sentinel-2 reference samples.

Sample	Lake Precision	Lake Recall	Lake F1 Score
George_VI_2018-02-04_1	1.00	1.00	1.00
George_VI_2018-02-04_2	1.00	1.00	1.00
George_VI_2020-01-19_1	0.97	0.95	0.95
George_VI_2020-01-19_2	1.00	1.00	1.00
George_VI_2020-01-19_3	0.99	0.93	0.96
George_VI_2020-01-19_4	1.00	1.00	1.00
George_VI_2020-01-19_5	1.00	1.00	1.00
George_VI_2021-01-23	0.96	0.90	0.93
Bach_2021-01-23	1.00	1.00	1.00
Amery_2020-02-17	1.00	1.00	1.00
Amery_2019-01-13_1	0.95	0.94	0.94
Amery_2019-01-13_2	0.96	0.95	0.96
Amery_2019-02-22	1.00	0.93	0.96
Riiser_Larsen_2019-02-17_1	1.00	1.00	1.00
Riiser_Larsen_2019-02-17_2	1.00	1.00	1.00
Roi Baudouin_2020-01-29_1	1.00	1.00	1.00
Roi Baudouin_2020-01-29_2	1.00	1.00	1.00
Roi Baudouin_2018-02-06	0.97	0.91	0.92
Roi Baudouin_2020-01-18	1.00	1.00	1.00

Representative Sentinel-2 classification results are presented in Fig. S1 of the Supplementary Information.

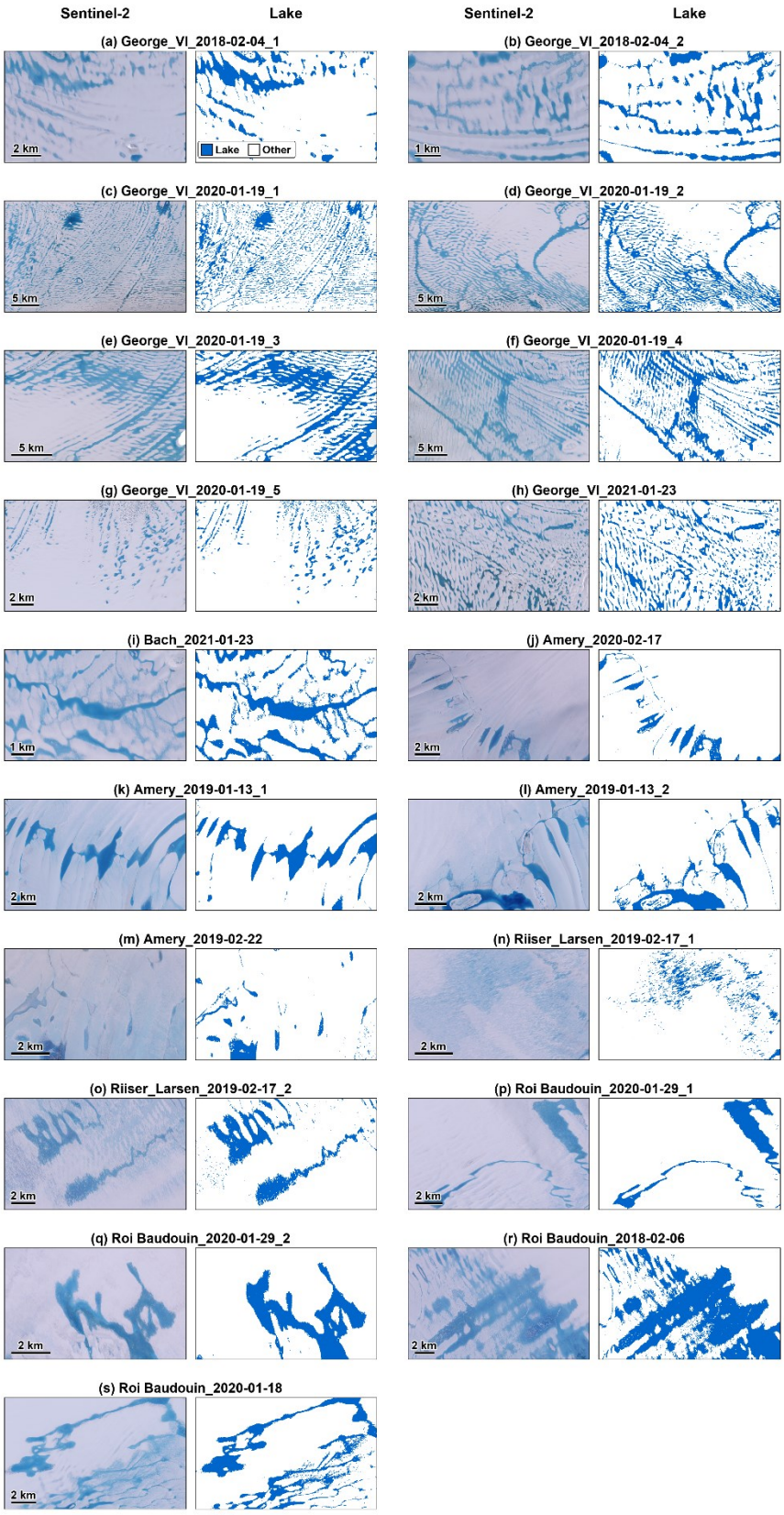


Figure S1: SGL extraction results from Sentinel-2 imagery. (a)–(s) show the true-color Sentinel-2 images and corresponding binary classification maps for the 19 Sentinel-2 image samples used in model cross-validation.

4.The authors need to check all the references they have used to support statements in the Introduction. Many are inappropriate because they refer to regions other than Antarctica, or to papers in which completely different methods were used from those suggested. There are also many recent papers that are highly relevant but are not cited. I have given more details on these in the line-by-line comments below.

AR5: Thank you for this important comment. We acknowledge that some references in the original Introduction were not sufficiently relevant to the Antarctic context or did not adequately support the corresponding statements. In response, we have carefully reviewed and revised the references throughout the Introduction, replacing less relevant citations with studies that more directly support the corresponding scientific statements.

We particularly appreciate the reviewer's recommendations of relevant studies, which have helped us strengthen the scientific background and improve the quality of the manuscript. The specific changes to the references and corresponding text are detailed in our responses to the line-by-line comments below.

5.I'm not convinced the melt flux dataset of Zheng et al. as used is providing a sensible constraint. It appears individual melt flux values from SSM/I on specific days are used to constrain the optical ponding data. But passive microwave sensors are incredibly sensitive to the instantaneous presence of liquid water within the near-surface snow/firn matrix. As soon as the surface temperatures drop and freezing begins, that liquid water refreezes or stays trapped. SSM/I will instantly register zero active melt flux.

However, SGLs that filled during peak melt days do not simply vanish when active melting stops. Because of the sheer thermal mass of deep water and the ice's topography, surface lakes can persist for days or weeks after active melt flux drops to zero. An optical satellite image taken on a cold, non-melting day will still show massive, clear blue water ponding.

Another way to use Zheng et al. (2025) would be to use it as a cumulative lag constraint. You could:

• Calculate Cumulative Melt Energy: Integrate Zheng et al.'s daily melt flux over a rolling window (e.g., a 3-day, 5-day, or 10-day antecedent period) leading up to the optical image acquisition date.

• Establish a Threshold: If the cumulative melt flux over the previous week is zero, and your optical imagery claims there are lakes, you can confidently flag those optical pixels as false positives (such as cloud shadows or blue ice exposures mistranslated as water).

• Identify Lake Drainage Events: If Zheng et al. show massive active melt flux for 5 days, but your subsequent optical imagery shows zero water ponding, it provides a strong proxy indicator that a hydrofracture or a rapid subglacial lake drainage event occurred.

AR6: We appreciate your detailed comment regarding the use of surface melt flux as a constraint. We agree that SGLs may persist after active melting ceases and that daily melt flux should not be used as a direct indicator of lake presence. We acknowledge that our original manuscript did not clearly describe the actual implementation of the melt constraint.

Our original method already considers this temporal mismatch by using three consecutive 8-day periods, rather than relying on melt flux from individual days or a single 8-day period. Specifically, for each MOD09A1 composite, daily melt flux from Zheng et al. (2025) is accumulated separately over the preceding, corresponding, and following 8-day periods. A pixel satisfies the melt condition if the cumulative melt exceeds 0.32 mm in any one of these periods. This approach allows for a temporal offset between surface melting and lake observations, reducing the risk of excluding lakes that persist after active melting has ceased.

Furthermore, MOD09A1 is an 8-day composite product that selects the best available observation for each pixel. Although observation dates are available at the native 500 m resolution, our study aggregates these observations to 1 km using mean aggregation, meaning that individual 1 km pixels may combine reflectance measurements acquired on different days. Therefore, applying a pixel-specific cumulative melt constraint over a fixed number of preceding days would require additional assumptions about the representative observation date. Our three-period approach is designed to accommodate this temporal variability while remaining consistent with the 8-day resolution of the dataset.

We recognize that some lakes may persist beyond these time windows and that melt flux alone cannot reliably identify lake drainage events. Therefore, the melt mask is used only as an auxiliary constraint rather than a direct indicator of lake presence or drainage. We have revised Sect. 3.7 to accurately describe the method already used in our study and clarify its limitations. The corresponding revisions to Sect. 3.7 are detailed in **AR3.**

6.There are several places in the text and on figures where I would recommend writing out the names ‘Roi Baudoin’ and ‘Nivlison’ in full instead of using

abbreviations. This seems especially relevant given that Tracy Tremenchus is written in full.

AR7: This is an excellent suggestion, and we appreciate you raising it. We agree that using the full names of the ice shelves improves clarity and consistency throughout the manuscript. We have therefore replaced the abbreviated names with their full forms throughout the main text, tables, and figure labels and captions, specifically replacing "Nivl" with "Nivlisen" and "Baudouin" with "Roi Baudouin".

7.I appreciate this is a methods paper, but as a glaciologist, I was disappointed that the paper did not discuss any of the glaciological implications of the findings or compare the findings with results of similar previous work. For example, how do the persistency statistics compare with previous work? How does the statistic of 65% of water appearing within 10 km of the grounding line compare? Where is the rest of the water, i.e. what percentage is more than 10 km above the grounding line versus more than 10 km below it? What have you been able to say with this new dataset about water ponding on ice shelves that has not been said before?

AR8: We appreciate your valuable comment. We agree that the glaciological implications of our findings and comparisons with previous studies were insufficiently discussed in the original manuscript. To address this, we have expanded Sects. 4.2–4.4 to compare our findings on SGL persistence, spatial distribution, and seasonal variability with previous studies and briefly discuss their glaciological implications.

In particular, we have provided additional statistics on SGL distributions relative to grounding lines, including the proportions located on grounded ice and floating ice shelves within and beyond 10 km of grounding lines (Fig. S3). We have also expanded the discussion of potential mechanisms underlying the concentration of SGLs near grounding lines, including upstream meltwater transport, accumulation in topographic depressions, and enhanced surface melting associated with katabatic winds and low-albedo blue ice.

As ESSD primarily focuses on the description and evaluation of datasets, we have kept these discussions concise while providing additional scientific context for interpreting and using the dataset.

The corresponding discussions have been revised in Sects. 4.2–4.4 of the manuscript.

> Overall, Antarctic SGLs exhibit predominantly low persistence and pronounced regional differences. Shen et al. (2025) similarly found that most Antarctic SGL

pixels have low annual recurrence, with frequently recurring lakes concentrated near grounding lines. Dirscherl et al. (2021) also identified recurrent lake formation over 4–5 years in localized depressions on East Antarctic ice shelves. While previous studies primarily examined the recurrence of SGLs across different years, our study further quantifies their persistence within individual melt seasons using 8-day observations, revealing their intermittent occurrence at a finer temporal scale. Specifically, approximately 83% of SGL pixels have mean persistence rates below 5%, while relatively persistent lake occurrence is concentrated in parts of East Antarctica and the Antarctic Peninsula. This indicates that widespread intermittent ponding coexists with localized areas of more frequent lake occurrence. By quantifying these patterns across 23 melt seasons at 8-day resolution, the dataset provides a basis for distinguishing persistent and intermittent surface ponding regimes and investigating their implications for Antarctic surface hydrology. **(L314–323)**

Overall, the spatial distribution of Antarctic SGLs is broadly consistent with previous studies. East Antarctica accounts for approximately 80% of the total SGL area, closely matching the 79% reported by Shen et al. (2025). The concentration of lakes near grounding lines also agrees with Stokes et al. (2019) and Corr et al. (2022), the latter reporting that 56.4% of open-water area in West Antarctica and the Antarctic Peninsula occurred within 1 km of grounding lines. This pattern may partly reflect the transport of meltwater from upstream grounded ice onto flatter ice-shelf surfaces, where it accumulates in topographic depressions (Kingslake et al., 2017; Lenaerts et al., 2017). In some East Antarctic grounding zones, persistent katabatic winds can also enhance near-surface warming and erode snow, exposing low-albedo blue ice that promotes further melting (Lenaerts et al., 2017; Stokes et al., 2019). These processes may help explain the observed concentration of SGLs near grounding lines and blue-ice areas. However, the proportion of SGL area on ice shelves estimated here (~60%) is lower than the values of 81.6%, 79%, and 70% reported by Stokes et al. (2019), Shen et al. (2025), and Tuckett et al. (2025), respectively, potentially reflecting differences in study regions, observation periods, and mapped water types. These spatial patterns provide a basis for investigating surface meltwater accumulation, transport, and potential hydrofracture susceptibility across Antarctica. **(L358–369)**

The pronounced interannual variability in Antarctic SGL area (CV = 0.48) is

consistent with previous studies. Arthur et al. (2022) reported SGL volume anomalies exceeding 200% on individual East Antarctic ice shelves and asynchronous peak years among different ice shelves. Similarly, Tuckett et al. (2025) found that mean annual surface meltwater area in East Antarctica during 2014–2021 was more than twice that during 2007–2013. The seasonal pattern identified here, characterized by lake expansion during December, a maximum in January, and subsequent decline, also agrees with previous observations (Dirscherl et al., 2021; Tuckett et al., 2025). Beyond these established patterns, the 23-year record further quantifies differences in the timing of seasonal SGL development across Antarctica. In particular, SGL area generally peaks in early January in West Antarctica, mid-January in East Antarctica, and late January to early February on the Antarctic Peninsula. This staggered seasonal progression indicates that peak surface ponding does not occur simultaneously across Antarctica, providing a more detailed temporal basis for investigating regional differences in meltwater accumulation and their relationships with atmospheric and surface conditions. **(L411–421)**

The newly added reference is as follows:

Arthur, J. F., Stokes, C. R., Jamieson, S. S. R., Carr, J. R., Leeson, A. A., and Verjans, V.: Large interannual variability in supraglacial lakes around East Antarctica, Nature Communications, 13, 1711, https://doi.org/10.1038/s41467-022-29385-3, 2022.

Dirscherl, M. C., Dietz, A. J., and Kuenzer, C.: Seasonal evolution of Antarctic supraglacial lakes in 2015–2021 and links to environmental controls, The Cryosphere, 15, 5205–5226, https://doi.org/10.5194/tc-15-5205-2021, 2021.

Shen, X.-Y., Ke, C.-Q., Li, H.-L., Cai, Y., Xiao, Y., and Li, M.-M.: Evolution of supraglacial lakes over the pan-Antarctic ice sheet between 2014 and 2022: Assessment and the control factors, Advances in Climate Change Research, 16, 337–349, https://doi.org/10.1016/j.accre.2025.02.005, 2025.

We have also added statistics on the remaining SGL distribution beyond 10 km from the grounding lines, as presented in Fig. S3 of the Supplement.

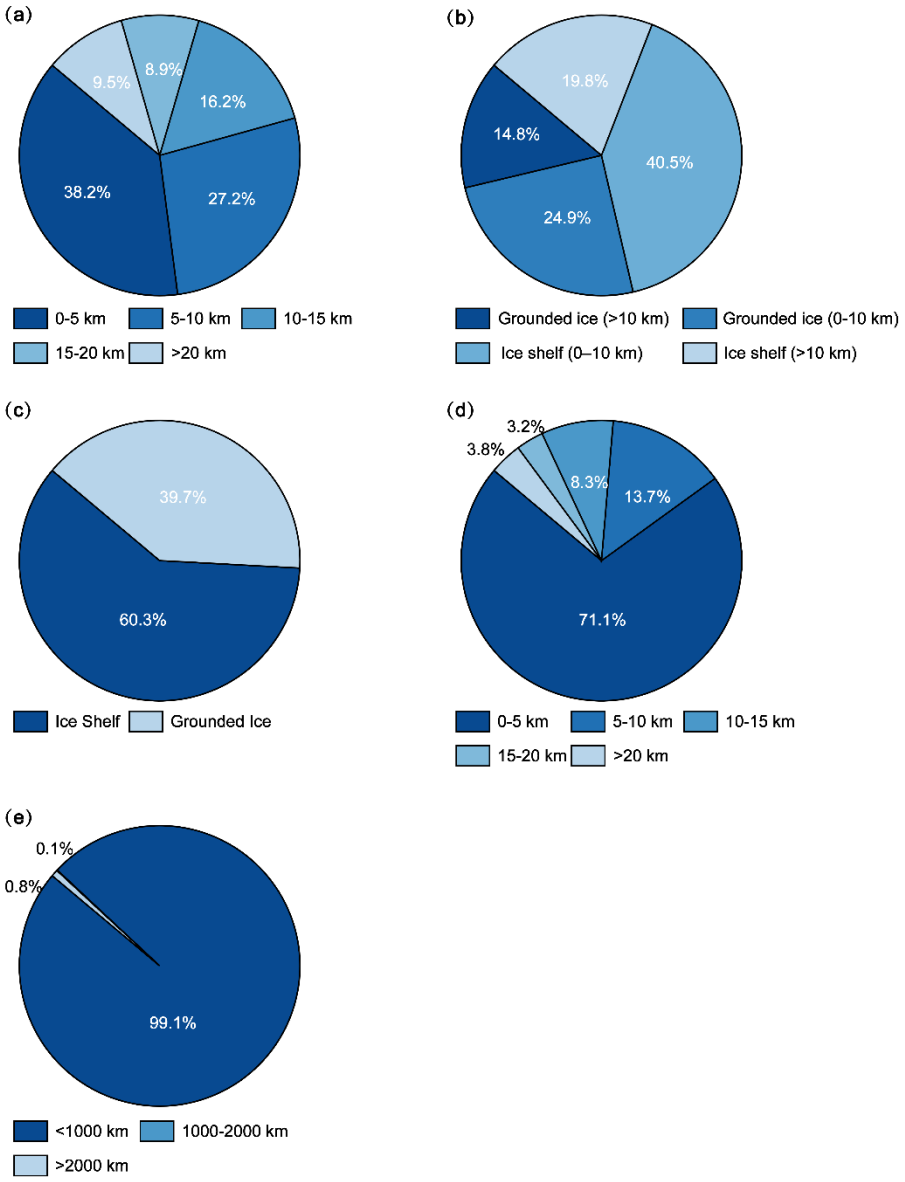


Figure S3: Percentage distribution of the multiyear mean maximum SGL area across Antarctica under different spatial conditions. (a) Distribution between grounded ice and ice shelves; (b) surface elevation; (c) distance to grounding lines; (d) distribution across grounded ice and floating ice shelves at different distances from grounding lines; and (e) distance to blue-ice areas and exposed bedrock.

Minor comments

1. L15. Could you incorporate some information about how the persistence rate was calculated? Depending on how much space you have in the abstract, you could write "… approximately 83% of lakes exhibit a multi-year mean persistence rate below 5%, appearing in fewer than one out of twenty 8-day observations per melt season." Or,

more briefly, "… with approximately 83% of lakes exhibiting a mean seasonal observation persistence below 5% across the 23-year record."

AR9: Thank you for this helpful suggestion. We have revised the Abstract to clarify how SGL persistence is calculated.

The corresponding sentence has been revised in the Abstract, as follows:

> The dataset reveals highly intermittent lake occurrence, with approximately 83% of SGL pixels exhibiting mean persistence rates below 5% across 23 melt seasons, based on the ratio of observations with detected SGLs to the total number of observations within each melt season. **(L15–18)**

2.L27. Echelmeyer et al. (1991) is the wrong reference because it concerns the Greenland Ice Sheet, not the Antarctic Ice Sheet.

AR10: Thank you for pointing this out. We agree that the study by Echelmeyer et al. (1991) focuses on the Greenland Ice Sheet and is not appropriate for supporting this statement about Antarctica. We have removed this reference and replaced it with studies that directly address Antarctic surface melting and supraglacial lake formation.

The corresponding sentence has been revised in the Introduction.

> As the climate warms, rising air temperatures can enhance surface melting in Antarctica, promoting the accumulation of meltwater within topographic lows on impermeable ice surfaces and the formation of supraglacial lakes (SGLs) (Dirscherl et al., 2021; Stokes et al., 2019; Trusel et al., 2015). **(L27–30)**

The newly added reference is as follows:

> Dirscherl, M. C., Dietz, A. J., and Kuenzer, C.: Seasonal evolution of Antarctic supraglacial lakes in 2015–2021 and links to environmental controls, The Cryosphere, 15, 5205–5226, https://doi.org/10.5194/tc-15-5205-2021, 2021.

3.L29–30. Lüthje et al. (2006) and Tedesco et al. (2012) concern the Greenland Ice Sheet, not the Antarctic Ice Sheet. You could either make the sentence refer more generically to ice sheets and/or retain the reference to Antarctica and substitute a more relevant reference, e.g.: Dell, R. L., Willis, I. C., Arnold, N. S., Banwell, A. F., & de Roda Husman, S. (2024). Substantial contribution of slush to meltwater area across Antarctic ice shelves. Nature Geoscience, 17(7), 624–630. This paper explicitly links surface water to albedo reduction.

AR11: We agree that Lüthje et al. (2006) and Tedesco et al. (2012) focus on the

Greenland Ice Sheet and are not appropriate references for this statement about Antarctica. We have removed these references and incorporated the recommended study by Dell et al. (2024). We have also revised the sentence to better reflect this process.

The corresponding sentence has been revised in the Introduction.

> SGLs lower surface albedo, enhance solar energy absorption, and promote further surface melting through positive melt–albedo feedback (Dell et al., 2024). **(L32–33)**

The newly added reference is as follows:

> Dell, R. L., Willis, I. C., Arnold, N. S., Banwell, A. F., and de Roda Husman, S.: Substantial contribution of slush to meltwater area across Antarctic ice shelves, Nature Geoscience, 17, 624–630, https://doi.org/10.1038/s41561-024-01466-6, 2024.

4. L31–32. All these references concern Greenland. I am not aware of any published study currently showing that lake drainage on Antarctic Peninsula glaciers causes glacier acceleration. There are a few studies measuring seasonal variations in velocity from satellites and suggesting that these may be due to meltwater penetrating to the bed, e.g.:

Boxall, K., Christie, F. D. W., Willis, I. C., Wuite, J. & Nagler, T. Seasonal land-ice-flow variability in the Antarctic Peninsula. The Cryosphere, 16, 3907–3932 (2022).

Wallis, B. J., Hogg, A. E., van Wessem, J. M., Davison, B. J. & van den Broeke, M. R. Widespread seasonal speed-up of west Antarctic Peninsula glaciers from 2014 to 2021. Nature Geoscience, 16, 231–237 (2023).

There is also a recent study measuring in situ acceleration in response to rainfall events:

Sugiyama, S., Kondo, K., Minowa, M. et al. Acceleration of an Antarctic outlet glacier driven by surface meltwater input to the base. Nature Communications, 17, 6102 (2026).

AR12: We are grateful for your insightful comments and for bringing these relevant studies to our attention. We agree that the original references did not adequately support the statement about glacier acceleration on the Antarctic Peninsula.

We have revised the text to distinguish between direct evidence of meltwater-driven

glacier acceleration and observed seasonal variations in ice flow. Specifically, we have added recent studies from Greenland and East Antarctica that provide evidence of the influence of surface meltwater on glacier dynamics. For the Antarctic Peninsula, we have incorporated the recommended studies by Boxall et al. (2022) and Wallis et al. (2023), while clarifying that the observed seasonal glacier speed-ups may be associated with surface meltwater input and other environmental factors.

The corresponding description has been revised in the Introduction.

> Surface meltwater reaching the glacier bed can increase subglacial water pressure and accelerate ice flow, as observed in Greenland (Das et al., 2008; Gjerde et al., 2025; Tedesco et al., 2013; Wei et al., 2026a) and more recently in East Antarctica (Sugiyama et al., 2026). Satellite observations have also revealed seasonal glacier speed-ups on the Antarctic Peninsula, potentially associated with surface meltwater input and other environmental factors (Boxall et al., 2022; Wallis et al., 2023). **(L33–37)**

The newly added references are as follows:

> Boxall, K., Christie, F. D. W., Willis, I. C., Wuite, J., and Nagler, T.: Seasonal land-ice-flow variability in the Antarctic Peninsula, The Cryosphere, 16, 3907–3932, https://doi.org/10.5194/tc-16-3907-2022, 2022.
>
> Gjerde, G., Behn, M. D., Stevens, L. A., Das, S. B., and Joughin, I.: Seasonal drainage-system evolution beneath the Greenland Ice Sheet inferred from transient speed-up events, The Cryosphere, 19, 6149–6169, https://doi.org/10.5194/tc-19-6149-2025, 2025.
>
> Sugiyama, S., Kondo, K., Minowa, M., and Watanabe, A.: Acceleration of an Antarctic outlet glacier driven by surface meltwater input to the base, Nature Communications, 17, 6102, https://doi.org/10.1038/s41467-026-72724-x, 2026.
>
> Wallis, B. J., Hogg, A. E., van Wessem, J. M., Davison, B. J., and van den Broeke, M. R.: Widespread seasonal speed-up of west Antarctic Peninsula glaciers from 2014 to 2021, Nature Geoscience, 16, 231–237, https://doi.org/10.1038/s41561-023-01131-4, 2023.
>
> Wei, J., Yang, K., Zhu, Y., Wang, Y., and Guo, X.: Satellite monitoring of Greenland wintertime buried lake drainage and potential ice flow response, Remote Sensing of Environment, 333, 115157,

https://doi.org/10.1016/j.rse.2025.115157, 2026.

5. L37–38. There are many other references that could be cited here besides Niu et al. (2023), and at least some deserve to be acknowledged.

AR13: We agree that the original citation did not adequately reflect the range of previous studies on Antarctic SGL monitoring. We have therefore expanded the references to include Arthur et al. (2020), Dirscherl et al. (2021), Stokes et al. (2019), and Tuckett et al. (2025), alongside Niu et al. (2023).

The corresponding sentence has been revised in the Introduction.

Remote sensing provides an effective approach for investigating the spatial distribution and temporal evolution of SGLs in Antarctica (Arthur et al., 2020; Dirscherl et al., 2021; Niu et al., 2023; Stokes et al., 2019; Tuckett et al., 2025). **(L42–43)**

The newly added reference is as follows:

Dirscherl, M. C., Dietz, A. J., and Kuenzer, C.: Seasonal evolution of Antarctic supraglacial lakes in 2015–2021 and links to environmental controls, The Cryosphere, 15, 5205–5226, https://doi.org/10.5194/tc-15-5205-2021, 2021.

6. L39. None of these references concern Antarctica. The reference for the Pamir seems particularly misplaced. You should refer to some of the many papers that have used Sentinel or Landsat data for Antarctica, e.g.:

Dirscherl, M. C., Dietz, A. J., and Kuenzer, C.: Seasonal evolution of Antarctic supraglacial lakes in 2015–2021 and links to environmental controls, The Cryosphere, 15, 5205–5226, https://doi.org/10.5194/tc-15-5205-2021, 2021.

Moussavi, M., Pope, A., Halberstadt, A. R. W., Trusel, L. D., Ciomi, L., and Abdalati, W. (2020). Antarctic Supraglacial Lake Detection Using Landsat 8 and Sentinel-2 Imagery: Towards Continental Generation of Lake Volumes. Remote Sensing, 12(1), 134.

Koehler, J., Baumhoer, C., Wouters, B., Lhermitte, S., and Dietz, A. Advancing supraglacial lake mapping in Antarctica: A deep learning approach using Sentinel-2 imagery. Environmental Data Science, 5, e38 (2026). https://doi.org/10.1017/eds.2026.10065.

Tuckett, P. A., Ely, J. C., Sole, A. J., Lea, J. M., Livingstone, S. J., Jones, J. M., and van Wessem, J. M.: Automated mapping of the seasonal evolution of surface meltwater and its links to climate on the Amery Ice Shelf, Antarctica, The Cryosphere,

15, 5785–5804, https://doi.org/10.5194/tc-15-5785-2021, 2021.

Halberstadt, A. R. W., Gleason, C. J., Moussavi, M. S., Pope, A., Trusel, L. D., and DeConto, R. M. (2020). Antarctic Supraglacial Lake Identification Using Landsat-8 Image Classification. Remote Sensing, 12(8), 1327. https://doi.org/10.3390/rs12081327.

Dell, R. L., Banwell, A. F., Willis, I. C., Arnold, N. S., Halberstadt, A. R. W., Chudley, T. R., and Pritchard, H. D. (2022). Supervised classification of slush and ponded water on Antarctic ice shelves using Landsat 8 imagery. Journal of Glaciology, 68(268), 401–414. https://doi.org/10.1017/jog.2021.114.

AR14: Thank you for providing relevant references. We agree that the original citations were not sufficiently relevant to Antarctic SGL monitoring. We have therefore reviewed and replaced them with studies that specifically investigate Antarctic surface water using optical satellite imagery, including the recommended studies by Dell et al. (2022), Halberstadt et al. (2020), and Koehler et al. (2026). We have also added the spatial resolution ranges of the satellite sensors to improve the clarity of the description.

The corresponding sentence has been revised in the Introduction.

> High-spatial-resolution optical satellite data, such as Landsat (15–100 m), Sentinel-2 (10–60 m), and WorldView (0.3–30 m), are widely used for SGL monitoring (Dell et al., 2022; Halberstadt et al., 2020; Kingslake et al., 2017; Koehler et al., 2026; Moussavi et al., 2020). **(L43–46)**

The newly added references are as follows:

> Dell, R. L., Banwell, A. F., Willis, I. C., Arnold, N. S., Halberstadt, A. R. W., Chudley, T. R., and Pritchard, H. D.: Supervised classification of slush and ponded water on Antarctic ice shelves using Landsat 8 imagery, Journal of Glaciology, 68, 401–414, https://doi.org/10.1017/jog.2021.114, 2022.
>
> Halberstadt, A. R. W., Gleason, C. J., Moussavi, M. S., Pope, A., Trusel, L. D., and DeConto, R. M.: Antarctic Supraglacial Lake Identification Using Landsat-8 Image Classification, Remote Sensing, 12, 1327, https://doi.org/10.3390/rs12081327, 2020.
>
> Koehler, J., Baumhoer, C., Wouters, B., Lhermitte, S., and Dietz, A.: Advancing supraglacial lake mapping in Antarctica: A deep learning approach using Sentinel-2 imagery, Environmental Data Science, 5, e38,

https://doi.org/10.1017/eds.2026.10065, 2026.

7. L44–45 and L48–49. Some of these references are completely inappropriate here. Most use either the wrong methodology or concern the wrong continent.

AR15: We appreciate you pointing out that these references were not appropriate in this context. We agree that some of the original citations did not adequately support the statements regarding Antarctic SGL monitoring and the limitations of moderate-resolution satellite imagery.

We have carefully reviewed and updated the references to ensure their relevance to the study region and methods discussed. Specifically, we have incorporated studies using MODIS imagery to investigate Antarctic SGLs and revised the citations supporting the discussion of mixed-pixel effects.

The corresponding descriptions have been revised in the Introduction.

> To improve temporal coverage, medium- to low-resolution satellite imagery, such as data from the Moderate Resolution Imaging Spectroradiometer (MODIS; 250–1000 m), has been used for SGL monitoring due to its high revisit frequency (Arthur et al., 2020; Hubbard et al., 2016; MacDonald et al., 2019; Spergel et al., 2021). **(L49–51)**

> This mixed-pixel effect can introduce biases in lake area estimates and reduce the detectability of small or narrow water bodies, limiting the ability of moderate-resolution sensors to accurately characterize the full range of SGL sizes (Arthur et al., 2020; Dirscherl et al., 2021). **(L53–55)**

The newly added references are as follows:

> Dirscherl, M. C., Dietz, A. J., and Kuenzer, C.: Seasonal evolution of Antarctic supraglacial lakes in 2015–2021 and links to environmental controls, The Cryosphere, 15, 5205–5226, https://doi.org/10.5194/tc-15-5205-2021, 2021.
>
> MacDonald, G. J., Banwell, A. F., Willis, I. C., Mayer, D. P., Goodsell, B., and MacAyeal, D. R.: Formation of pedestalled, relict lakes on the McMurdo Ice Shelf, Antarctica, Journal of Glaciology, 65, 337–343, https://doi.org/10.1017/jog.2019.17, 2019.
>
> Spergel, J. J., Kingslake, J., Creyts, T., van Wessem, M., and Fricker, H. A.: Surface meltwater drainage and ponding on Amery Ice Shelf, East Antarctica, 1973–2019, Journal of Glaciology, 67, 985–998,

https://doi.org/10.1017/jog.2021.46, 2021.

8. L52. This is the first mention of 'SGL fraction'. I suggest explicitly defining what you mean here. Is this at the pixel scale?

AR16: Thank you for this helpful suggestion. We agree that the term "SGL fraction" should be clearly defined when first introduced.

The corresponding description has been revised in the Introduction.

> In this study, a new Antarctic SGL fraction dataset derived from MODIS imagery is presented. SGL fraction is defined as the proportion of each 1 km grid cell covered by supraglacial lakes, with values ranging from 0 to 1. **(L58–59)**

9. L92–93. State why surface slope is required. Why and how is it used?

AR17: We have clarified the purpose and application of surface slope in our study. Specifically, slope information is used as an auxiliary terrain constraint to exclude steep areas where topographic shadows may be misclassified as SGLs. The detailed screening criteria are provided in Sect. 3.5 (see **AR3**).

The corresponding description has been revised in Sect. 2.3, Auxiliary data.

> Surface slope is calculated from the CryoSat-2 digital elevation model (DEM) at 1 km spatial resolution (Slater et al., 2018) and is used to exclude steep terrain during SGL candidate screening, thereby reducing false detections caused by topographic shadows. **(L104–106)**

10. L93. The Slater et al. reference is not in the reference list.

AR18: Thank you for pointing out this omission. We have added the missing reference for the CryoSat-2 DEM (Slater et al., 2018) to the reference list of the revised manuscript.

The added reference is as follows:

> Slater, T., Shepherd, A., McMillan, M., Muir, A., Gilbert, L., Hogg, A. E., Konrad, H., and Parrinello, T.: A new digital elevation model of Antarctica derived from CryoSat-2 altimetry, The Cryosphere, 12, 1551–1562, https://doi.org/10.5194/tc-12-1551-2018, 2018.

11. L95–97. State briefly why and how these two datasets are used.

AR19: We consider this a valuable recommendation. We have revised the description

to clarify the purpose and application of both auxiliary datasets.

The corresponding description has been revised in Sect. 2.3, Auxiliary data.

> To further constrain the SGL mapping results, two independent datasets are incorporated: (1) a daily Antarctic melt-flux dataset (Zheng et al., 2025), which is used to generate melt masks as a physical constraint on SGL mapping, and (2) an existing Antarctic SGL dataset (Tuckett et al., 2025), which is used to derive the historical maximum lake extent for identifying potential misclassifications. **(L109–112)**

12. L98–99. You need to make it clear that you are working at the 1 km MODIS resolution here, I assume, rather than at the Sentinel-2 resolution.

AR20: Thank you for this suggestion. We agree that the spatial resolution should be explicitly stated to avoid confusion with the Sentinel-2 reference data. We have revised the description to clarify that SGL fraction retrieval is performed at the 1 km MODIS pixel scale, where individual pixels may contain mixtures of lake, snow, and ice.

The corresponding sentence has been revised in Sect. 3, Methods.

> Due to the relatively coarse spatial resolution of MODIS imagery, individual pixels often contain mixtures of lake and surrounding snow or ice, making it necessary to estimate the SGL fraction within each 1 km MODIS grid cell to accurately characterize SGL coverage across Antarctica. **(L114–116)**

13. L103. Put 'ground truth' in quotation marks because it is not strictly ground-based data.

AR21: We agree that the term "ground truth" is not strictly accurate for reference data derived from satellite imagery. We have therefore placed "ground-truth" in quotation marks to acknowledge this distinction.

The corresponding sentence has been revised in Sect. 3, Methods.

> The first component comprises four stages for constructing "ground-truth" datasets from Sentinel-2 imagery and developing the RFC and RFR models using daily MOD09GA surface reflectance data. **(L121–123)**

14. L106–112. These lines repeat L98–104. I suggest deleting L98–104

AR22: Thank you for pointing out this redundancy. We have removed the redundant

text to avoid repetition and improve the clarity and conciseness of the Methods section.

15. L129. When you say 'MODIS pixel scale', I assume you mean the resampled MODIS scale, i.e. 1 km. Your references to 1 km and 'MODIS pixel scale' here are ambiguous.

AR23: Thank you for pointing out this ambiguity. We have revised the description to explicitly state that the aggregation is performed at the 1 km resolution used in our machine-learning models.

The corresponding description has been revised in Sect. 3.1, Lake extraction from Sentinel-2 imagery.

> To match the 1 km spatial resolution of MODIS imagery used in the machine-learning models, two aggregation strategies are applied. First, max aggregation is used to generate binary SGL labels at 1 km resolution. **(L146–147)**

16. Fig. 2. Box 1 on the left and Box 2 on the right contain the spelling mistake 'extreation'.

AR24: Thank you for pointing out these typographical errors. We have corrected the spelling mistake "extreation" in Box 1 on the left and Box 2 on the right of Fig. 2.

The corrections have been made in Fig. 2 of the revised manuscript, as shown below:

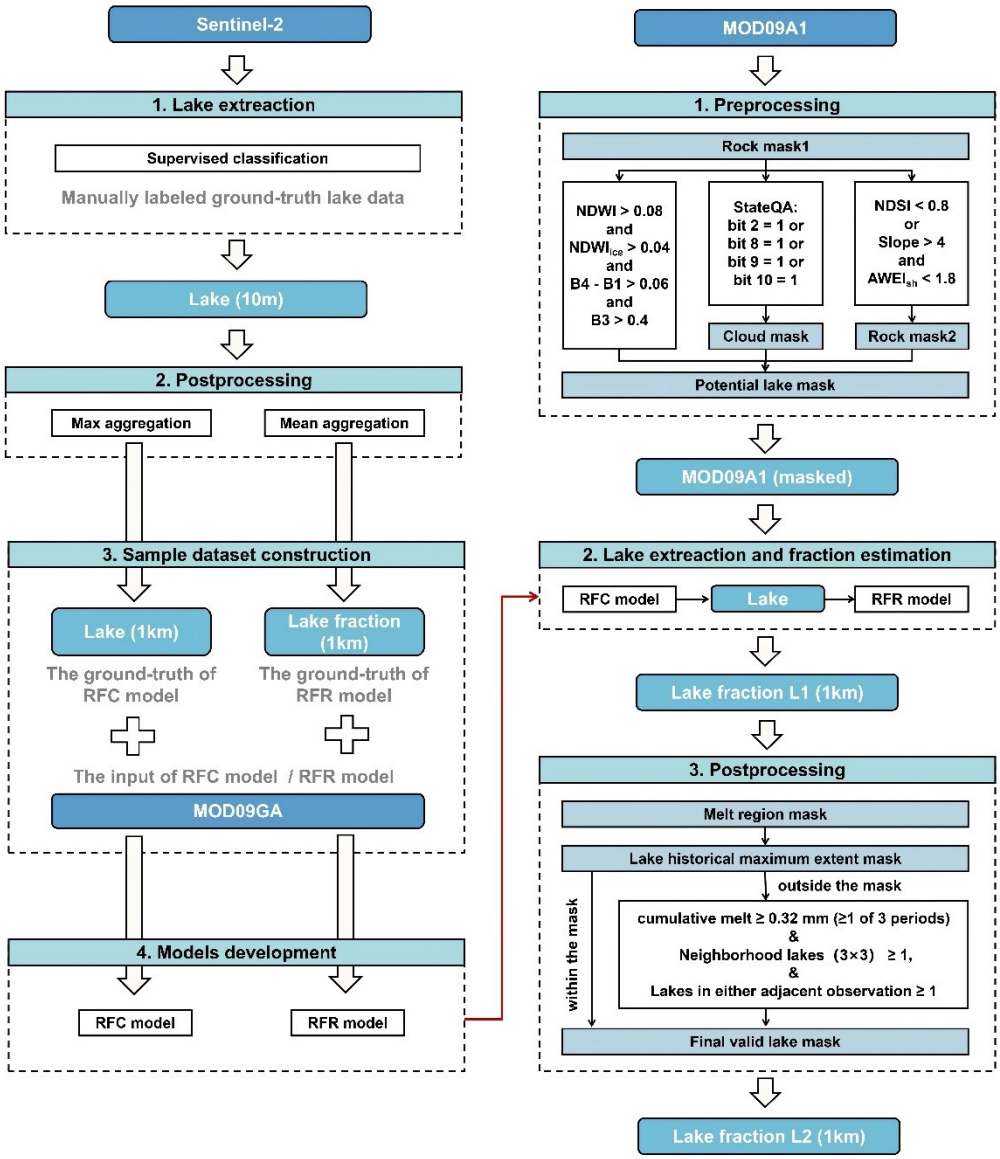


Figure 2: Workflow of the Antarctic SGL fraction dataset generation from Sentinel-2 and MODIS imagery.

17. L136. Again, when you say 'MODIS SGL pixels', are you working at 500 m or 1 km?

800 **AR25:** We agree that the original description did not clearly distinguish between the native 500 m MODIS resolution and the 1 km resolution used in our study. The original sentence was removed during the reorganization of the Methods section.

To avoid further confusion, we have clarified in Sect. 2.1 that both MOD09GA and MOD09A1 are resampled to 1 km using mean aggregation. We also explicitly state that all subsequent references to MODIS pixels refer to the 1 km resolution unless otherwise specified. In addition, we have reviewed the manuscript to ensure that

spatial resolution is clearly indicated where necessary.

The corresponding description has been revised in Sect. 2.1, MODIS surface reflectance data.

> To improve retrieval robustness and reduce sensitivity to noise and residual cloud contamination, both MOD09GA and MOD09A1 are resampled to a common spatial resolution of 1 km using mean aggregation (hereafter, all MODIS pixels refer to 1 km pixels unless otherwise specified). **(L72–74)**

18. L138. "…mixed surface signals within individual pixels" is unclear. Unless I have misunderstood, your 1 km MODIS pixels are made up of 100 × 10 m Sentinel-2 pixels. The whole point is that your 1 km pixels are likely to contain a mixture of 'water' and 'non-water' Sentinel-2 pixels.

AR26: We appreciate the additional context you provided. We agree that the original expression "mixed surface signals" was too vague. We have revised the description to explicitly explain that individual 1 km MODIS pixels may contain both lake water and surrounding snow or ice. This mixed-pixel effect is the primary motivation for estimating SGL fractions rather than relying solely on binary lake classification.

The corresponding sentence has been revised in Sect. 3, Methods.

> Due to the relatively coarse spatial resolution of MODIS imagery, individual pixels often contain mixtures of lake and surrounding snow or ice, making it necessary to estimate the SGL fraction within each 1 km MODIS grid cell to accurately characterize SGL coverage across Antarctica. **(L114–116)**

19. L172. Clarify what is meant by 'continuous' here. Across space, time, or both?

AR27: We agree that the term "continuous" was ambiguous in the original manuscript. Our intended meaning was that SGL fraction is a continuous variable ranging from 0 to 1, not that the term refers to spatial or temporal continuity. To avoid ambiguity, we have removed the term "continuous" from the revised manuscript and clarified the range of the RFR output.

The corresponding sentence has been revised in Sect. 3.4, Random forest model development and optimization.

> The RFR model produces SGL fraction estimates ranging from 0 to 1. **(L212–213)**

20.L188–189. I find the statement "…they are conditionally retained when both

spatial and temporal consistency criteria are satisfied (Fig. 2)" unclear. Fig. 2 refers to "neighbourhood lakes (3 × 3) ≥ 1" and "Lakes in either adjacent observation ≥ 1". I think this procedure needs to be explained more clearly. See my Main Point 2.

AR28: Thank you for this helpful comment. We agree that the original description of the spatial and temporal consistency criteria was insufficiently clear. We have expanded the explanation to specify how these criteria are applied to candidate SGL pixels outside the historical maximum lake extent.

Specifically, the spatial criterion requires at least one neighboring lake pixel within a 3 × 3 neighborhood, while the temporal criterion requires the target pixel to be identified as a lake in either the preceding or following 8-day observation. We have also clarified that these pixels are retained only when both consistency criteria and the surface melt condition are satisfied. These revisions provide a clearer description of the postprocessing procedure and its relationship to Fig. 2.

The corresponding revisions are provided in Sect. 3.7 (see **AR3**).

21.L178–189. Further to the above, I find it difficult to reconcile what is written in this section with the 'postprocessing' workflow box depicted in Fig. 2. See my Main Point 2.

AR29: Thank you for this comment. We agree that the original description was not sufficiently consistent with the postprocessing workflow shown in Fig. 2. We have therefore revised and expanded Sect. 3.7 to clarify the application of the surface melt constraint, historical lake extent mask, and spatial and temporal consistency criteria.

Please refer to **AR3** for the detailed revisions.

22. L195–196. I assume you are using 'validation' and 'evaluation' to mean the same thing here? I assume this cross-validation stage uses only the 19 calibration images mentioned on L132 and not the 7 validation images mentioned on L133. Please clarify this.

AR30: Thank you for this comment. We agree that the original description did not clearly distinguish between five-fold cross-validation and independent testing. We have revised the text to clarify that five-fold cross-validation is performed using samples from the 19 regions selected for model development, while samples from the remaining seven spatially independent regions are used exclusively for independent testing.

We have also clarified that "evaluation" refers to the assessment of model

performance, whereas "validation" refers to the validation subset used in each cross-validation fold. The independent test samples are not included in the cross-validation process.

The corresponding description has been revised in Sect. 4.1, Accuracy assessment.

> The performance of the RFC and RFR models is initially evaluated through five-fold cross-validation using datasets from 19 regions. The samples are divided into five approximately equal subsets. In each iteration, four subsets are used for training, while the remaining subset is used for validation. **(L240–242)**

> To further assess model transferability, independent tests are conducted using seven samples from spatially distinct regions of Antarctica, covering multiple melt seasons from 2017 to 2020 (Fig. 1 and Table 2). **(L254–255)**

23. Figs. 7 and 8. Earlier in the paper you mention where the rock dataset comes from, but I do not think you mention the source of the blue-ice dataset. It would be useful to put the source of both datasets in the figure captions.

AR31: Thank you for this helpful suggestion. We agree that the sources of the exposed bedrock and blue-ice datasets should be clearly identified. We have therefore added a reference to the source of the blue-ice data in Sect. 2.3 and updated the captions of Figs. 7 and 8 to explicitly acknowledge both datasets.

The corresponding description has been added to Sect. 2.3, Auxiliary data, as follows:

> To minimize misclassification between SGLs and other surface features, exposed bedrock polygons from the ADD are applied as a spatial mask. **(L103–104)**

> Blue-ice areas are obtained from the Antarctic surface cover dataset (Hui et al., 2014) for subsequent analysis of the spatial distribution of SGLs in relation to blue-ice areas. **(L108–109)**

The caption of Fig. 7 has been revised as follows:

> Figure 7: Multi-year mean persistence of SGLs across Antarctica (2000–2023). (a) Amery Ice Shelf; (b) Nivlisen Ice Shelf; (c) Tracy Tremenchus Ice Shelf; (d) Riiser-Larsen Ice Shelf; (e) Roi Baudouin Ice Shelf; (f) Thwaites Ice Shelf; (g) Voyeykov Ice Shelf; (h) George VI Ice Shelf; (i) regional summary of multi-year mean SGL persistence. The radius of each pie chart represents the multi-year mean maximum SGL area of the corresponding region. Exposed bedrock data are obtained from the ADD, while blue-ice data are obtained from the Antarctic

surface cover dataset (Hui et al., 2014). **(L296–301)**

The caption of Fig. 8 has been revised as follows:

Figure 8: Mean annual SGL fraction across Antarctica (2000–2023). (a) Amery Ice Shelf; (b) Nivlisen Ice Shelf; (c) Tracy Tremenchus Ice Shelf; (d) Riiser-Larsen Ice Shelf; (e) Roi Baudouin Ice Shelf; (f) Thwaites Ice Shelf; (g) Voyeykov Ice Shelf; (h) George VI Ice Shelf; (i) regional statistics of multi-year
910 mean maximum SGL area. Each pie chart radius represents the multi-year mean maximum SGL area. Exposed bedrock data are obtained from the ADD, while blue-ice data are obtained from the Antarctic surface cover dataset (Hui et al., 2014). **(L336–340)**

The added reference is as follows:

Hui, F., Ci, T., Cheng, X., Scambos, T. A., Liu, Y., Zhang, Y., Chi, Z., Huang, H., Wang, X., Wang, F., Zhao, C., Jin, Z., and Wang, K.: Mapping blue-ice areas in Antarctica using ETM+ and MODIS data, Annals of Glaciology, 55, 129–137, https://doi.org/10.3189/2014AoG66A069, 2014.